Base-Case Model for Measurement Uncertainty in a Reverberation Chamber Including Frequency Stirring

Angelo Gifuni, *Member, IEEE,* Luca Bastianelli, Franco Moglie, *Senior Member, IEEE,* Valter Mariani Primiani, *Senior Member, IEEE,* and Gabriele Gradoni, *Member, IEEE*

***Abstract*— We address the uncertainty of reverberation chamber measurements in presence of both mechanical and frequency stirring (FS). A base-case model is derived for reverberation fields affected by the measurement uncertainty due to the lack of a perfect statistical uniformity of fields in a reverberation chamber (RC). It is found that the measurement uncertainty associated with the FS depends on both the total uncorrelated samples and the local insertion loss (IL). The local IL depends on the frequency stirring bandwidth (FSB). The model allows for obtaining separate measurement uncertainty contributions. Measurements support the achieved uncertainty model. In particular, results show that the dependence on the IL is normally rather weak also when very wide FSBs are used.**

***Index Terms*— Reverberation chamber, mechanical stirring, frequency stirring, measurement uncertainty, uncertainty quantification.**

I Introduction

COMBINATION of stirring techniques, i.e., hybrid stirring, is very important for reverberation chambers (RCs) as it increases the number of uncorrelated samples and, consequently, it reduces the measurement uncertainty [1]-[15]; it facilitates the development of applications for RCs [1]-[16]. The most ordinary combinations of stirring techniques include the frequency stirring (FS) [1]-[9], [11]-[14]. Originally, the FS was introduced in [17]; then it was gradually developed into more systematic studies [18], [19] and applied to electromagnetic compatibility (EMC) tests [19]. In this paper, a combination of mechanical and frequency stirring is considered, where mechanical stirring (MS) is realized by using both a metallic stirrer(s) and platform stirring; the latter, which can be obtained by a manual position stirring, is equivalent to source stirring. Here, the position of an antenna includes its orientation and polarization; that is, a change of position of the antenna can be achieved by the change of its location, orientation, and/or of its polarization. A proper combination of MS mechanisms neutralizes the effects of any field non-uniformity [10], [13, sec. II *C*]. In principle, the measurement uncertainty component due to the non-uniformity can be partly reduced by FS choosing an appropriate bandwidth; however, such a reduction is only marginal. The measurement uncertainty in RCs, when both MS and FS are used, is discussed in [13] and [15]; it is also formally addressed by a statistical test in [12]. To the best of our knowledge, a statistical model, which allows for separately and deductively obtaining contributions from the total measurement uncertainty, is not present in literature. The aim of this work is to develop and verify this model. It is found that measurement uncertainty due to the frequency stirring depends not only on the number of total uncorrelated samples, but also on the local trend of the insertion loss (IL) of an RC. The local IL depends on the frequency stirring bandwidth (FSB), which is denoted by Δf; and the corresponding central frequency is denoted by f_0. Note that here the word "samples" identifies a sequence or a set of structured sequences (hybrid stirring) of RVs. In this paper, the IL measurement is considered; however, the results can be extended for different measurements made in an RC [12]-[13] or for measurements obtained by a combination of ILs. Note that the IL is equal to the net transfer function defined in [2], when it is corrected for mismatches of the two antennas. The measurement uncertainty model is first developed for well-stirred fields and then expanded to include imperfectly stirred reverberation fields. It is specified that when the physical quantity to be measured is not constant through Δf, then the model includes the measurement uncertainty due to the fact that the value of the IL may not correspond to the value of IL at central frequency f_0 [20]; that is, the result is given as an average value in Δf. This is the case assumed here. The paper is organized as follows: in section II the theory is shown; in section III, experimental results are shown; in section IV, results are discussed and conclusions are drawn.

Manuscript received July, 31 2017; revised September, 11 2017 and October, 06 2017.

A. Gifuni is with the Dipartimento di Ingegneria, Universita di Napoli ` Parthenope, Centro Direzionale di Napoli, Napoli 80143, Italy (e-mail: angelo. gifuni@uniparthenope.it).

L. Bastianelli, F. Moglie, and V.M. Primiani are with the Dipartimento di Ingegneria dell'Informazione, Universita Politecnica delle Marche, 60131 Ancona, Italy (e-mail: f.moglie@univpm.it; l.bastianelli@pm.univpm.it; v.mariani@univpm.it).

G. Gradoni is with the School of Mathematical Sciences and with the George Green Institute for Electromagnetics Research, Department of Electrical and Electronics Engineering, University of Nottingham, Nottingham NG7 2RD, U.K. (e-mail: gabriele.gradoni@nottingham. ac.uk).

II Measurement uncertainty Model for Hybrid Mechanical and Frequency Stirring

When the samples are acquired at a single frequency and the stirring is only mechanical, e.g., operated through metallic stirrer(s) only, it can be written as

$$IL = \left\langle \left| S_{21} \right|^2 \right\rangle_N , \quad (1)$$

where $< >_N$ represents the ensemble average with respect to the N uncorrelated field configurations in the chamber. Actually, IL is a sample mean (SM) and therefore has statistical fluctuations: it is a random variable (RV). The parameter $<|S_{21}|^2>_N$ can be considered both uncorrected and corrected for mismatches and radiation efficiencies of the antennas. For corrected measurements, the type of distribution of the IL is not changed; however, the variations of the relevant parameters (mean and variance) have to be considered [21]. By considering the common dimensions of the RCs, well-stirred fields, whose distribution is well known [22], are normally achieved in the GHz range. At frequencies less than one GHz, the fields are not well stirred as both the cavity modal density and the stirring efficiency are low. Consequentially, the corresponding distribution deviates from the idealized asymptotic distribution [4]. Similarly, the field uniformity degrades.

A. Case of well-stirred fields

We first consider an ideal RC, whose Cartesian fields are well fitted by the statistics of a perfectly uniform and isotropic random fields. By considering the well-known distribution of $|S_{21}|^2$ [4], [22], we can write the mean, variance, and variation coefficient (VC) of the RV IL_f, respectively, as follows:

$$\mu_{IL_f} = IL_{f,0} , \quad (2)$$

$$\sigma^2_{IL_f} = \frac{\left(IL_{f,0} \right)^2}{N} , \quad (3)$$

$$\delta^2_{IL_f} = \frac{\sigma^2_{IL_f}}{\left(IL_{f,0} \right)^2} = \frac{1}{N} , \quad (4)$$

where N is the number of uncorrelated samples used to estimate the SMs, IL_f, and f is the frequency. When the samples are acquired both by mechanical and frequency stirring, then (1) can be expressed by a double ensemble average, as follows [13]:

$$IL_{N,\Delta f} = W = \left\langle \left\langle \left| S_{21} \right|^2 \right\rangle_N \right\rangle_k = IL_{\Delta f,N} = \left\langle \left\langle \left| S_{21} \right|^2 \right\rangle_k \right\rangle_N , \quad (5)$$

where the subscript Δf means that the averages are made over k uncorrelated frequency samples in Δf; clearly, k is greater than one in presence of FS. Since the estimate of the average given by (5), as well as the estimate of the concerning measurement uncertainty, does not change when the averages with respect to N and k are exchanged, the two corresponding procedures to achieve the measurement uncertainty are very similar. In other words, the two procedures produce the same results. More specifically, if one considers the average with respect to k first, then some further mathematical steps are necessary at the beginning; the two procedures are exactly the same from (6) onwards. Here, we consider the averages with respect to N first and then those with respect to k. The averages for each frequency point correspond to SMs including only the MS. Such SMs are assumed to be uncorrelated RVs and they are denoted by IL_{f1}, IL_{f2}, ⋯, IL_{fk}. Their corresponding mean values are denoted by $IL_{f1,0}$, $IL_{f2,0}$, ⋯, $IL_{fk,0}$. Under the hypotheses made, any useful position of the antennas can be considered. The RV W given by (5) can be expressed as follows:

$$W = \frac{1}{k}\left[IL_{f1} + IL_{f2} + IL_{f3} + \cdots + IL_{fk} \right] . \quad (6)$$

Note that $\Delta f = f_k - f_1$, where f_1 and f_k are the minimum and the maximum frequency of the FS. We are interested in the mean and variance of W. We can write:

$$\mu_W = W_0 = \frac{1}{k}\left[IL_{f1,0} + IL_{f2,0} + IL_{f3,0} + \cdots + IL_{fk,0} \right] . \quad (7)$$

By combining (3) and (6), we can write:

$$\sigma^2_W = = \frac{1}{kN}\left\{ \frac{\left(IL_{f1,0} \right)^2 + \left(IL_{f2,0} \right)^2 + \left(IL_{f3,0} \right)^2 + \cdots + \left(IL_{fk,0} \right)^2}{k} \right\} . \quad (8)$$

Now, we want to transform (8) so that, when it is compared to (3), it gives a formal connection between MS and FS. In order to make such a comparison, we connect the quadratic mean $(W_0)^2$ to the mean square value (MSV) of the means $IL_{f1,0}$, $IL_{f2,0}$, ⋯, $IL_{fk,0}$, appearing in (8), whence [23]

$$\left(W_0 \right)^2 + \sigma^2_{\Delta f} = \left[\frac{\left(IL_{f1,0} \right)^2 + \left(IL_{f2,0} \right)^2 + \cdots + \left(IL_{fk,0} \right)^2}{k} \right] , \quad (9a)$$

$$\left(W_0 \right)^2 \left(1 + \delta^2_{\Delta f} \right) = \left[\frac{\left(IL_{f1,0} \right)^2 + \left(IL_{f2,0} \right)^2 + \cdots + \left(IL_{fk,0} \right)^2}{k} \right] , \quad (9b)$$

where $\sigma_{\Delta f}$ and $\delta_{\Delta f}$ are respectively the standard deviation and the VC of the means $IL_{f1,0}$, $IL_{f2,0}$, ⋯, $IL_{fk,0}$. Equations (9a) and (9b) are equivalent; they can both be used to quantify the measurement uncertainty from the hybrid stirring. By manipulating (8) and (9a) or (9b), we can write:

$$\sigma_W = \frac{W_0}{\sqrt{kN}} \sqrt{1 + \delta^2_{\Delta f}} . \quad (10)$$

Equation (10) can also be recast as follow:

$$\sigma_W = \frac{\sqrt{\left(W_0 \right)^2 + \sigma^2_{\Delta f}}}{\sqrt{kN}} . \quad (11)$$

By measurement of the IL of an RC at the sample frequencies f_i ($i = 1, 2, \ldots, k$) within the FSB, one can estimate the means $IL_{f1,0}$, $IL_{f2,0}$, ⋯, $IL_{fk,0}$, as well as $(W_0)^2$ and $\delta^2_{\Delta f}$. For applications, $\sigma^2_{\Delta f}$ is estimated by measurements as a sample variance. Then, by using (10), we can calculate the measurement uncertainty σ_W. If $IL_{f1,0}$ =

$IL_{f2,0} = IL_{f3,0} = \cdots = IL_{fk,0} = IL_{f,0} = \mu_W$, then $\delta^2_{\Delta f} = 0$ and both (8) and (10) give

$$\sigma_W = \frac{W_0}{\sqrt{kN}}. \tag{12}$$

Using (10) and (12) yields

$$\delta_W = \frac{\sqrt{1+\delta^2_{\Delta f}}}{\sqrt{kN}}, \tag{13}$$

which becomes minimum when $\delta^2_{\Delta f} = 0$. For k = 1, the achieved model retrieves the pure MS model of (3) and (4), of which it is an extension. Note that the result (10) and (13) implies the validity of (8), i.e., the application of (10) and (13) implies that the minimum sample size N be such that a reasonable estimate of the quadratic means $(IL_{f1,0})^2$, $(IL_{f2,0})^2$, $\cdots$, $(IL_{fk,0})^2$ is obtained. The sample size N, as well as k, affects the measurements uncertainty of the estimates of W_0 and $\delta^2_{\Delta f}$; but, N and k do not affect such uncertainties in the same way. Moreover, (9) can be actually written for any $N \geq 1$, by replacing the means squared on the right side with the single amplitudes squared of the coefficient S_{21}. It is important to note that N does not affect the mean of W whereas k affects it. In other words, the population of W is formed of different subpopulations, whose number is equal to k. Strictly, the means of the single subpopulations are different each other. It will be seen that results from measurements are acceptable when N is greater than or equal to 4, an empirical value observed in different RC facilities, which gives an acceptable statistical estimate for the model derived in the paper [24], [25]. In any case, it is worth to be noticed that the VC $\delta_{\Delta f}$ increases as N decreases. To the limit of $N = 1$, $\delta_{\Delta f}$ turns out to be maximum; that is, it turns out that $\delta_{\Delta f} \cong 1$. If (10) and (13) are applied to a real RC, operated with MS through metallic stirrer(s), the measurement uncertainty contribution due to the lack of a perfect uniformity is not taken into account. On the other hand, those formulas are inadequate to be applied for a real RC, where a hybrid mechanical, but not frequency, stirring is present (both metallic stirrer(s) and position stirrer(s)). Nevertheless, (10) and (13) can be confirmed experimentally, if the RC fields are perfectly stirred and statistically uniform. If we now consider p independent positions of at least one of the two antennas in a real RC, where statistical anisotropy and non-uniformity are affecting the reverberation field, then we can write:

$$W_{mp} = \frac{1}{p}\left[W_{sp,1} + W_{sp,2} + \cdots + W_{sp,p}\right], \tag{14}$$

$$\sigma^2_{W_{sp,i}} = \frac{\left(W_{sp,i,0}\right)^2}{kN}\left(1+\delta^2_{\Delta f,sp,i}\right) + \sigma^2_{sp,p} \quad (i = 1, 2, \cdots, p), \tag{15}$$

where the subscripts p, i, mp, and sp mean p positions, i-th position, multiple positions, and a single position; $\sigma^2_{W_{sp,i}}$ is the variance of W_{sp} at the i-th position; $W_{sp,i,0}$ is the mean of $W_{sp,i}$; $\delta_{\Delta f,sp,i}$ is the VC referred to the i-th position; $\sigma^2_{sp,p}$ is the variance due to the lack of perfect uniformity for any i-th W_{sp} calculated for p positions, which *de facto* corresponds to $\sigma^2_{G_{ref},p}$ in [11] when it is estimated by measurements. According to (14) and (15), (5) should be rewritten by adding an external average with respect to p. We can write:

$$W_{mp,0} = \frac{1}{p}\left[W_{sp,1,0} + W_{sp,2,0} + \cdots + W_{sp,p,0}\right], \tag{16}$$

$$\sigma^2_{W_{mp}} = \frac{1}{p}\left\{\begin{aligned}&\left[\frac{\left(W_{sp,1,0}\right)^2}{pkN}\left(1+\delta^2_{\Delta f,sp,1}\right) + \frac{\left(W_{sp,2,0}\right)^2}{pkN}\left(1+\delta^2_{\Delta f,sp,2}\right)\right.\\ &\left.+\cdots+\frac{\left(W_{sp,p,0}\right)^2}{pkN}\left(1+\delta^2_{\Delta f,sp,p}\right)\right]\\ &+\sigma^2_{sp,p}\end{aligned}\right\}. \tag{17}$$

Furthermore, by using (17), we can write:

$$\sigma^2_{W_{mp}} = \left\{\begin{aligned}&\frac{\left(1+\delta^2_{\Delta f}\right)}{pkN}\left[\frac{\left(W_{sp,1,0}\right)^2 + \left(W_{sp,2,0}\right)^2 + \cdots + \left(W_{sp,p,0}\right)^2}{p}\right]\\ &+\frac{\sigma^2_{sp,p}}{p}\end{aligned}\right\}, \tag{18}$$

$$\sigma^2_{W_{mp}} = \frac{W^2_{mp,0}}{pkN}\left(1+\delta^2_{sp,p}\right)\left(1+\delta^2_{\Delta f}\right) + \frac{\sigma^2_{sp,p}}{p}, \tag{19}$$

where $\delta_{\Delta f,sp,i}$ is assumed to be constant and denoted by $\delta_{\Delta f}$, and $\delta^2_{sp,p} = \sigma^2_{sp,p} / W^2_{mp,0}$. In experimental applications, $\sigma^2_{\Delta f}$ and $\sigma^2_{sp,p}$ are estimated by measurements as sample variances. Note that it is implicitly assumed $p > 4$ [24], [25]. The first term on the right side of (19) expresses an accurate form of the measurement uncertainty contribution depending on the number of uncorrelated samples pkN, $\delta_{sp,p}$, and to $\delta_{\Delta f}$; the last two parameters depend on the local trend of the ILs. The first term on the right side of (19) is normally less than the second term for loaded RCs, except the cases where kN is not very large [12]-[13]. This is quantitatively shown in the section III in this paper. If k = 1 (only MS), then (19), becomes as follows:

$$\sigma^2_{W_{mp}} = \frac{W^2_{mp,0}}{pN}\left(1+\delta^2_{sp,p}\right) + \frac{\sigma^2_{sp,p}}{p}. \tag{20}$$

It is useful to write (19) as follows:

$$\sigma^2_{W_{mp}} = \frac{W^2_{mp,0}}{pkN} CF + \frac{\sigma^2_{sp,p}}{p}, \tag{21}$$

where

$$CF = \left(1+\delta^2_{\Delta f}\right)\left(1+\delta^2_{sp,p}\right). \tag{22}$$

We put for convenience:

$$R_{\delta sq} = \delta^2_{sp,p} / \delta^2_{\Delta f}. \tag{23}$$

If k = 1, then $CF = \left(1+\delta_{sp,p}^2\right)$ as (20) shows. If $R_\delta << 1$, then $CF \cong \left(1+\delta_{\Delta f}^2\right)$ and results turn out to be simplified. Finally, we can write:

$$\sigma_{W_{mp}} = \sqrt{\frac{W_{mp,0}^2}{pkN} CF + \frac{\sigma_{sp,p}^2}{p}} = \sqrt{\sigma_1^2 + \sigma_2^2} \,, \tag{24}$$

where

$$\sigma_1 = \frac{w_{mp,0}}{\sqrt{pkN}} \sqrt{CF} \,, \tag{25}$$

$$\sigma_2 = \frac{\sigma_{sp,p}}{\sqrt{p}} \,. \tag{26}$$

Equations (25) and (26) allow to estimate measurement uncertainty contributions σ_1 and σ_2; however, they are not completely uncorrelated as mentioned above. The total relative measurement uncertainty can be written as follows:

$$\delta_{W_{mp}} = \sqrt{\frac{CF}{pkN} + \frac{\sigma_{sp,p}^2}{W_{mp,0}^2 p}} = \sqrt{\frac{CF}{pkN} + \frac{\delta_{sp,p}^2}{p}} = \sqrt{\sigma_{1,r}^2 + \sigma_{2,r}^2} \,, \tag{27}$$

where $\sigma_{1,r}^2$ and $\sigma_{2,r}^2$ are the contributions to the relative measurement uncertainty, which correspond to the uncertainties squared σ_1^2 and σ_2^2. Similarly to (10) and (13), (24) and (27) give standard uncertainties. In section III, the validation for (24) and (27) are shown. Moreover, the necessary condition $\delta_{\Delta f,sp,i} \cong \delta_{\Delta f}$ is verified. The coefficient CF is estimated along with the ratio $R_{\delta sq}$, as well as the measurement uncertainty contributions $\sigma_{1,r}$ and $\sigma_{2,r}$ for given configurations of an RC.

B. Cases of imperfectly stirred fields

The models (10) and (24) can be derived when the coefficient of variation of the distribution of $\left|S_{21}\right|_{fi}^2 = E^2$ (i = 1, 2, ⋯, k), which is an exponential distribution, is constant as the frequency changes. This condition is hardly satisfied at low frequencies, especially as the RC excitation approaches the lowest usable frequency (LUF): the probability density function (PDF) of fields/power deviates from asymptotic predictions as the modal overlapping factor is reduced, which is the case at relatively low frequency operation of an RC [1], [26]-[31]. The PDF of E^2 is not fitted from an exponential when unstirred contributions are present in the RC [32]. Nevertheless, in [33] it is shown that the necessary condition on the VC to rigorously derive the models (10) and (24) is essentially satisfied in heavily loaded RCs. Imperfectly stirred fields could also be produced inside vibrating intrinsic RCs (VIRCs) [34]. The application of (10) and (24) can be forced, by using measurements at low frequencies, in order to estimate the goodness of the results in cases where the PDF of the IL could move from the exponential. Such an estimate is made and results are shown in the next section.

III RESULTS FROM MEASUREMENTS

In this section, (24), and (27) are validated by processing measured data from real RCs. Corrections for impedance mismatches are not necessary for such validations. Note that the validation requires measurements for a significant number of positions of the antennas. The measurements presented in this section are performed by manually changing location, as well as polarization, of the antennas. A possible degradation of the measurement calibration does not affect the procedure of validation. Actually, (10) and (13) are also separately validated first. The mean W_0 in (10) is estimated n times and the standard deviation of such n averages W_i (i = 1, 2, ⋯, n) is calculated. The calculated standard deviation is an estimate of the measured standard uncertainty. When such an uncertainty is normalized to the average of the averages W_i, an estimate of the relative standard uncertainty is obtained. The estimate of the measured standard uncertainty is compared to the corresponding expected standard uncertainty, which is obtained by applying (10) or equivalently (11). It is applied by using any of the n estimates W_i and the corresponding estimate of $\sigma_{\Delta f}^2$. Measurements are made in the RC at Università Politecnica delle Marche, Ancona, Italy, The RC is a rectangular chamber of 60 m^3 volume, where the input electromagnetic field is randomized by means of two metallic stirrers [35], which work in step mode for measurements used in this paper. The measurement setup includes a four-port VNA, model Agilent 5071B and two antennas, whose model is Schwarzbeck Mess-Elektronik USLP 9143, whose usable frequency range ranges from 250 MHz to 8 GHz for EMC tests. Measurements are acquired in the frequency range (FR) from 200 MHz to 8.2 GHz; by automation, 16000 samples are acquired for each position of the stirrers; the step frequency (SF) is 500 kHz. The IF bandwidth and source power, which determine the instrument measurement uncertainty along with the set FR and amplitude of the measured transmission coefficient, are set to 3 kHz and 0 dBm, respectively. The total number of stirrer positions, which corresponds to the total number of (frequency) sweeps (M) is 64. It is further specified that the total sweeps are divided in n sets of (frequency) sweeps, so that each set includes N sweeps and $M = n \cdot N$. The settings n and N are changed to test the model. For each sweep, the total number of frequency points K = 16000 is divided in q sets of frequencies, so that $\Delta f = (k - 1) \cdot$ SF and $K = k \cdot q$. The value of q is the number of FSB or Δf included in the FR. In order to show further information included in data, we also show the behaviour of (10) and (13) when W_0 and $\sigma_{\Delta f}^2$ are estimated by using all the available positions of the stirrers present in the measurements, as it can be seen below. The concerning uncertainties are called as further expected uncertainties in this paper. Considering the RC and the antennas, one notes that the start frequency is forced at the low frequencies, in order to test the model where the starting hypotheses are supposed not to be satisfied. By the autocorrelation function (ACF), it is verified that the

samples can be safely considered uncorrelated for the worst case at the frequency of 200 MHz. It is specified that both the non-correlation of the samples concerning the mechanical stirring and the one concerning the frequency stirring are verified by ACF. Many tests are made by using several combinations of N and k; all results obtained support the good agreement between predictions and measurements obtained with the uncertainty models (10) and (13). For sake of brevity, only the results for the case when k = 400, N = 8, and n = 8 are here reported in Fig. 1 and 2, for the measurement uncertainty and the relative measurement uncertainty given by (10) and (13), respectively. They also show the concerning further uncertainties; we reaffirm that such uncertainties are calculated by always using $M = N =$ 64. Note that $\Delta f = (k - 1) \cdot 0.5$ MHz = 199.5 MHz.

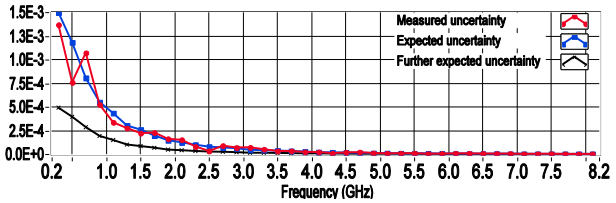

Fig. 1. Measurement uncertainty; for measured and expected uncertainties, M = 64, K = 16,000, N = 8, n = 8, and k = 400 (Δf = 199.5 MHz). For the further expected measurement uncertainty, W_0 and $\delta_{\Delta f}$ are obtained by using $N = M$ = 64.

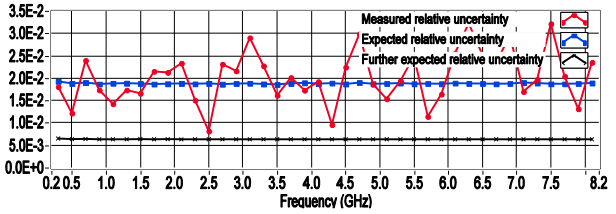

Fig. 2. Relative measurement uncertainty; for measured and expected relative uncertainties, M = 64, K = 16,000, N = 8, n = 8, and k = 400 (Δf = 199.5 MHz). For the further expected relative measurement uncertainty, W_0 and $\delta_{\Delta f}$ are obtained by using $N = M$ = 64.

We verified that measured and expected results match acceptably even reducing k, up to k = 4. It is also specified that results are confirmed when different RC test facilities are used. In fact, measurements from one of the two chambers at Universtà Parthenope of Naples, Naples, which works in step mode as well, are also used for such validations. Moreover, since the loading of an RC can change the local trend of its IL [36], measurements from chamber loaded by two pyramidal absorbers (Eccosorb VHP-8-NRL by Emerson & Cuming) are also considered. The max reduction of the IL caused by the load is of about 6.3 dB over the whole FR. Note that the frequency step was larger than the coherence bandwidth (CB) from 0.4 to 2.4 GHz for both empty and loaded chamber [37]. The load reduces the number of uncorrelated samples. In particular, the non-correlation condition is not satisfied for frequencies less than 300 MHz. By halving the frequency samples (SF = 1 MHz), the results appreciably improve in this band when the load is present in the RC. Hence, measured and expected uncertainties match also in presence of this loading. Overall, it can be safely stated that the use of different antennas for IL measurements [36] does not affect the applicability of the model; actually, the model includes the concerning measurement uncertainty. It is important to note that the results for the validation of (24) and (27) show experimental values of the VC $\delta_{\Delta f}$.

A. Results from Measurements for the validation of (24) and (27)

The validation of (24) and (27) implies a hard work in experimental measurements as mentioned above. We use 36 uncorrelated measurements of IL for the same amount of positions of the antennas. Location, orientation, and polarization of at least one of the two antennas are changed, so that the 36 uncorrelated IL measurements include such a spatial variation. The measurement settings are the same as in previous measurements. Therefore, FR ranges from 0.2 to 8.2 GHz; SF is 500 kHz, and the number of samples acquired for each sweep is 16,000. The total sweeps, which correspond to the same amount of mechanical positions of the stirrers, are M = 64. The number of sweeps $N \le M$ used for data processing and other setting such as k, and q are from time to time specified for results. The 36 measurements of IL are divided in 6 sets, so that each set includes 6 IL measurements (36 = 6 · 6). With reference to (14), p = 6. For any FSB, the average of the 6 ILs in each set is calculated, so that 6 uncorrelated estimates of $W_{mp,0}$ are obtained. The standard deviation of such 6 averages is the measured standard uncertainty. The estimate of the measured standard uncertainty is compared with the corresponding expected standard uncertainty, which is obtained by (24). It is obtained by using any of the 6 uncorrelated estimates of $W_{mp,0}$ and the corresponding estimates of $\delta_{\Delta f}$, $\sigma_{sp,p}$, and $\delta_{sp,p}$. The relative standard uncertainty is obtained by the concerning normalization of the standard uncertainty. The average of the 6 estimates of $W_{mp,0}$ is the further estimate of $W_{mp,0}$. Further estimates of the parameters $\sigma_{sp,p}$ and $\delta_{sp,p}$ are obtained by using all 36 available ILs concerning the positions of the antennas; therefore a further expected measurement uncertainty and concerning expected relative measurement uncertainty are obtained and shown. Note that $\delta_{\Delta f}$ is obtained by any of the 36 traces; it depends on N and Δf. Figures 3 and 4 show the VC $\delta_{\Delta f}$ for the 6 traces of the first set of IL measurements; in Fig. 3, N = 4, k = 40, and p = 6; in Fig. 4, $N = M$ = 64, k = 400, and p = 6. We extended the observed frequency range to the low frequency also in this measurement campaign. Note that k = 40 implies Δf = 19.5 MHz, which is a low FSB for common RCs; k = 400 implies Δf = 199.5 MHz, which is a significant FSB for common RCs. One can see that $\delta_{\Delta f}$ is sufficiently constant as the position of the antennas changes even for N = 4 and k = 40, except for f < 300 MHz. However, the necessary condition $\delta_{\Delta f,sp,i} \cong$ const. = $\delta_{\Delta f}$ for the mathematical step from (17) to (18) is practically satisfied for f > 250 MHz. Figure 5 shows the comparisons between the measured and expected uncertainties; Fig. 6 shows the comparisons between the measured and expected

relative uncertainties. In Figs. 5 and 6, N = 4, k = 40, and p = 6. Both Figs. 5 and 6 also show the further uncertainties. In Fig. 7, where N = 4, k = 40, and p = 6, the ratio $R_{\delta sq}$ is shown; in Fig. 7, the further ratio $R_{\delta sq}$ is also shown. Figure 8 shows the contributions $\sigma_{1,r}$ and $\sigma_{2,r}$ to the relative measurement uncertainty. Note that the further measured $\sigma_{2,r}$ is obtained by using all 36 available ILs. Clearly, $\sigma_{2,r}$ decreases as p increases.

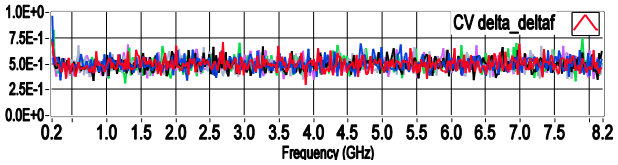

Fig. 3. VC $\delta_{\Delta f}$; 6 traces for the same amount of antenna positions; N = 4, k = 40 (19.5 MHz), and p = 6.

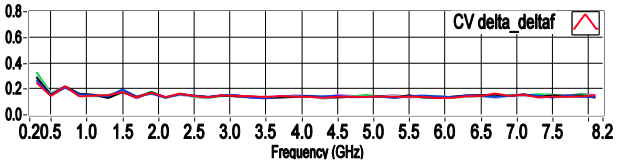

Fig. 4. VC $\delta_{\Delta f}$; 6 traces for the same amount of antenna positions; N = 64, k = 400 (199.5 MHz), and p = 6.

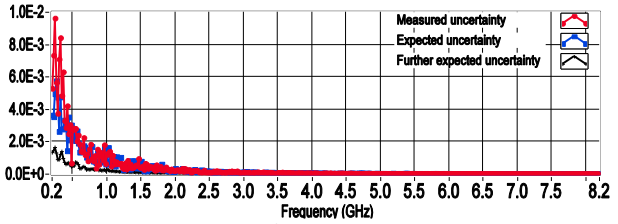

Fig. 5. Measurement uncertainty; for measured and expected uncertainties, N = 4, k = 40 (19.5 MHz), and p = 6. For the further expected measurement uncertainty, N = 64, k = 40, and p = 36.

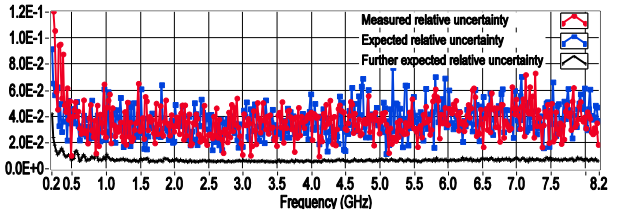

Fig. 6. Relative measurement uncertainty; for measured and expected relative uncertainties, N = 4, k = 40 (19.5 MHz), and p = 6. For the further expected relative measurement uncertainty, N = 64, k = 40, and p = 36.

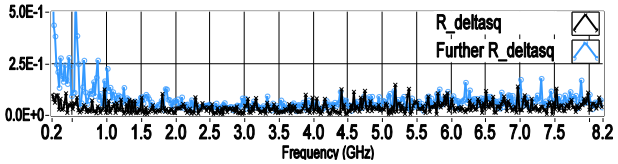

Fig. 7. Ratio $R_{\delta sq}$; for $R_{\delta sq}$, N = 4, k = 40 (19.5 MHz), and p = 6. For further $R_{\delta sq}$, N = 64, k = 40, and p = 36.

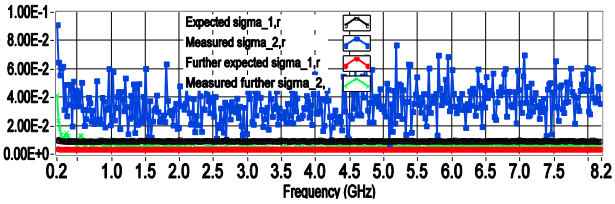

Fig. 8. Contributions $\sigma_{1,r}$ and $\sigma_{2,r}$ to the relative measurement uncertainty; N = 4, k = 40 (19.5 MHz), and p = 6; for further $\sigma_{1,r}$ and $\sigma_{2,r}$, N = 64, k = 40, and p = 36.

Figs. 9-12 show results corresponding to Figs. 5-8 where all processing settings are the same, except for N, which is equal to M = 64, and k = 400.

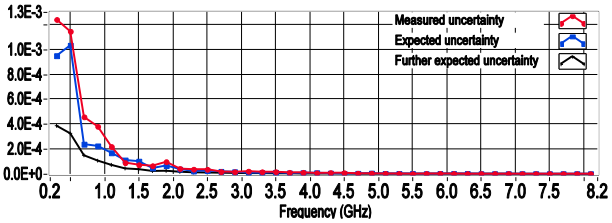

Fig. 9. Measurement uncertainty. All processing settings are the same as in Fig. 5, except for N = 64 and k = 400 (Δf = 199.5 MHz).

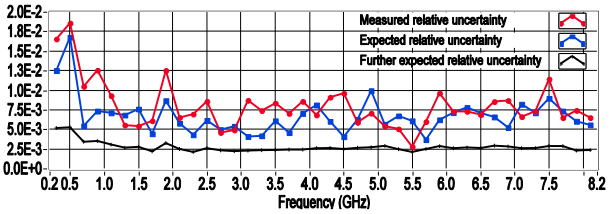

Fig. 10. Relative measurement uncertainty. All processing settings are the same as in Fig. 6, except for N = 64 and k = 400 (Δf = 199.5 MHz).

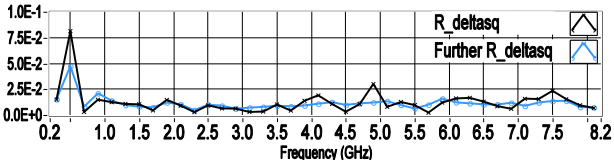

Fig. 11. Ratio $R_{\delta sq}$;. All processing settings are the same as in Fig. 7, except for N = 64 and k = 400 (Δf = 200 MHz).

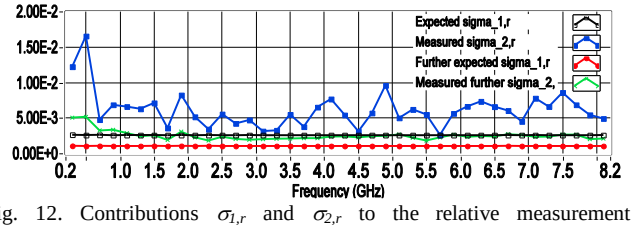

Fig. 12. Contributions $\sigma_{1,r}$ and $\sigma_{2,r}$ to the relative measurement uncertainty. All processing settings are the same as in Fig. 8, except for N = 64 and k = 400 (Δf = 199.5 MHz).

Results in Figs. 5 and 6, as well as those in Figs. 9 and 10, show that uncertainties measured and expected match well. Figs. 7 and 11 show that $\delta^2_{\Delta f}$ is greater than $\delta^2_{sp,p}$, when the RC is empty. Figs. 13-16 show the coefficient CF and the corresponding further CF. It is important to note that CF decreases as N increases. With reference to the empty RC, for N > 16 and k = 400 (Δf = 199.5 MHz), the effect of the

coefficient *CF* becomes negligible, as Figs. 15 shows. This result holds for Δf as wide as 395.5 MHz, as Fig. 16 shows.

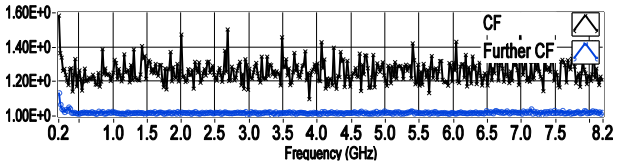

Fig. 13. Coefficient *CF*; for *CF*, N = 4, k = 40 (19.5 MHz), and p = 6; for further *CF*, N = 64, k = 40, and p = 36.

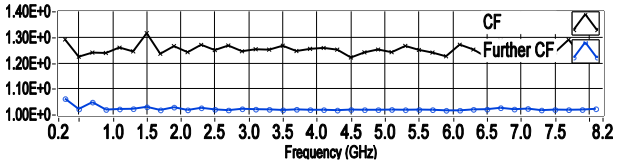

Fig. 14. Coefficient *CF*; for *CF*, N = 4, k = 400 (199.5 MHz), and p = 6; for further *CF*, N = 64, k = 400, and p = 36.

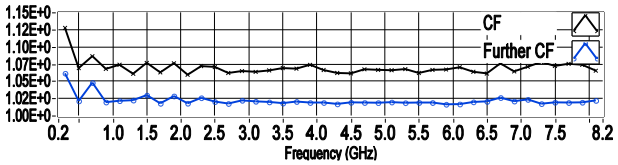

Fig. 15. Coefficient *CF*; for *CF*, N = 16, k = 400 (199.5 MHz), and p = 6; for further *CF*, M = N = 64, k = 400, and p = 36.

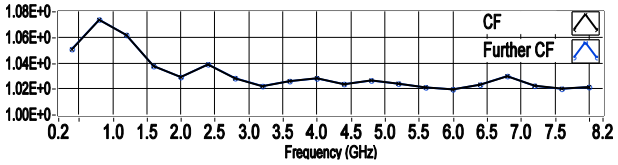

Fig. 16. Coefficient *CF*; for *CF*, N = 64, k = 800 (399.5 MHz), and p = 6; for further *CF*, N = 64, k = 800, and p = 36.

Figures 8 and 12 show that $\sigma_{2,r}$, which is the measurement uncertainty contribution due to the non-uniformity of fields in the RC, is generally greater that $\sigma_{1,r}$ when the RC is empty. It is specified that other tests are made by using several combinations of N and k; all results obtained support the measurement uncertainty model. Six measurements of ILs are made for the same amount of independent configurations of the loaded RC. The chamber is loaded by the two pyramidal absorbers; it is the same load mentioned above. The six independent configurations are obtained rearranging the positions of the absorbers and/or of the antennas. Figure 17 shows $\sigma_{1,r}$, where processing settings are similar to those in Fig. 12; Fig. 18 shows the frequency behavior of the coefficient *CF*, where processing settings are similar to those in Fig 15. However, results in Figs. 17 and 18 are achieved by abovementioned reduction (SF = 1 MHz).

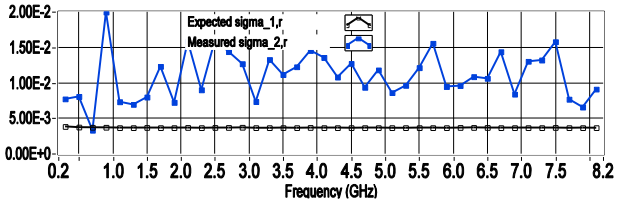

Fig. 17. Chamber loaded by two pyramidal absorbers. Contributions $\sigma_{1,r}$ and $\sigma_{2,r}$ to the relative measurement uncertainty; N = 64 and k = 200 (Δf = 199 MHz), and p = 6.

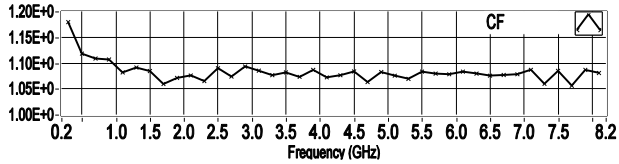

Fig. 18. Chamber loaded by two pyramidal absorbers. Coefficient *CF*; N = 16, k = 200 (199 MHz), and p = 6.

Since only six uncorrelated measurements of the loaded chamber are available, the further $\sigma_{1,r}$ and $\sigma_{2,r}$ are not shown in Fig. 17. By comparing the results in Figs. 12 and 17, it is noted that the difference between $\sigma_{2,r}$ and $\sigma_{1,r}$ significantly increases when the RC is loaded by the two pyramidal absorbers. It is important to stress that the difference between $\sigma_{1,r}$ and $\sigma_{2,r}$ depends on the ratio Nk/p. If Nk and p are of the same order of magnitude, then $\sigma_{1,r}$ is predominant. The coefficient *CF* is slightly increased under the effect of loading. However, it can be essentially neglected if compared with the other measurement uncertainty contributions. Similar results are found for $R_{\delta sq}$, which are not shown, again, for brevity. In other words, $\delta^2_{\Delta f}$ is greater than $\delta^2_{sp,p}$ when both the chamber is empty and loaded.

VI Discussion and Conclusions

We have shown a base-case model for the uncertainty of measurements made in an RC, which can be used when hybrid mechanical and frequency stirring are used, as well as when only MS is adopted, see (20). We find that the total measurement uncertainty is formed by two contributions: one contribution depends on the total number of uncorrelated samples and (less) on the coefficient *CF*; the other contribution depends on the lack of a perfect uniformity, which tends to increase under the effect of chamber loading. The coefficient *CF* depends on the local (frequency) behaviour of the insertion loss of an RC according to the FSB and on the lack of a perfect uniformity. Nevertheless, for both empty and loaded RC, it is found that such a dependence is typically weak, and when the total uncorrelated samples are much greater than one, the coefficient *CF* can be neglected and a simplified model can be used. The model allows us to easily verify the predominant uncertainty contribution by measurements for any condition of load in an RC. When the RC is strongly loaded, the contribution concerning the lack of a perfect uniformity tends to be predominant though, even if the other contribution is not negligible. In general conditions, the weight of each contribution to the total measurement uncertainty depends on the ratio Nk/p. Hence, the contribution due mainly to the total number of uncorrelated samples can become predominant when the samples are acquired in a way strongly spatial; that is, it can be predominant when Nk and p are of the same order of

magnitude. Strictly, the model is developed and valid under the condition of well-stirred fields in an RC. But, practically, it is verified that the results are acceptable also at relatively low frequencies, where the field is not well stirred. Since obtained measurement uncertainty is not much sensitive to changes to the PDF of the field in an RC, this implies moderate changes of the concerning VC. It is important to note that no difference is found on the measurement uncertainty when the order in the processing of the averages with respect to the mechanical and frequency stirring is inverted. In this paper, the central quantity from which we quantify the measurement uncertainty is the insertion loss; however, the results are consequential for different measurements made in an RC or for measurements obtained by a combination of ILs. Finally, it is important to note that the model is also applicable to mode-stirred RCs [38]-[40]; concerning results could be shown in a future publication.

REFERENCES

[1] IEC 61000-4-21, *Electromagnetic Compatibility (EMC)*, Part 4-21: Testing and measurement techniques – Reverberation chamber test methods, International Electrotechnical Commission, Geneva, Switzerland, 2011.

[2] U. Carlberg, P.-S. Kildal, A. Wolfang, O. Sotoudeh, C. Orlenius, "Calculated and measured absorption cross sections of lossy objects in reverberation chamber," *IEEE Trans. Electromagn. Compat.*, vol. 46, pp. 146-154, May 2004.

[3] U. Carlberg, P. S. Kildal, and J. Carlsson, "Numerical study of position stirring and frequency stirring in a loaded reverberation chamber," *IEEE Trans. Electromagn. Compat.*, vol. 51, pp. 12–17, 2009.

[4] D.A. Hill, *Electromagnetic Fields in Cavities: Deterministic and Statistical Theories*. New York: IEEE Press, 2009.

[5] C.L. Holloway, H.A. Haider, R.J. Pirkl, W.F. Yong, D.A. Hill, J. Ladbury, "Reverberation chamber techniques for determining the radiation and total efficiency of antennas," *IEEE Trans. Electromagn. Compat.*, vol.60, pp.1758-1770, April 2012.

[6] X. Chen "Measurement uncertainty of antenna efficiency in a Reverberation Chamber," *IEEE Trans. Electromagn. Compat.*, vol. 55, pp. 1331-1334, December 2013.

[7] C.L. Holloway, D.A. Hill, M. Sandroni, J. Ladbury, J. Coder, G. Koepke, A.C. Marvin, and Y. He, "Use of reverberation chambers to determine the shielding effectiveness of physically small, electrically large enclosures and cavities," *IEEE Trans. Electromagn. Compat.*, vol.50, pp. 770-782, November 2008.

[8] I.D. Flintoft, G.C. R. Melia, M.P. Robinson, J.F. Dawson, and A.C. Marvin, "Rapid and accurate broadband absorption cross-section measurement of human bodies in a reverberation chamber", *IOP Measurement Science and Technology*, vol. 26, no. 6, art. no. 065701, pp. 1-9, May 2015.

[9] A. Gifuni, I.D. Flintoft, Simon J. Bale, G.C. R. Melia, and A.C. Marvin, "A theory of alternative methods for measurements of absorption cross section and antenna radiation efficiency using nested and contiguous reverberation chambers", *IEEE Trans. Electromagn. Compat.*, vol. 58, pp. 678-685, 2016.

[10] A. Gifuni, G. Ferrara, A. Sorrentino, and M. Migliaccio, "Analysis of the measurement uncertainty of the absorption cross section in a reverberation chamber", *IEEE Trans. Electromagn. Compat.*, vol. 57, no. 5, pp. 1262-1265, Oct. 2015.

[11] J.A. Den Toorn, K.A. Remley, C.L. Holloway, J.M. Ladbury, & C.M. Wang, "Proximity-effect test for lossy wireless-device measurements in reverberation chambers," *IET Sci., Meas. & Technol.*, vol. *9*, pp. 540-546, Nov. 2014.

[12] K. A. Remley, C.-M. Wang, R. J. Pirkl, A. T. Kirk, J. Aan Den Toorn, D. F. Williams, C. L. Holloway, J. A. Jargon, and P. D. Hale, "A significance test for reverberation-chamber measurement uncertainty in total radiated power of wireless devices," *IEEE Trans. Electromagn. Compat.*, vol. 58, no. 1, pp. 207–219, February, 2016.

[13] K.A. Remley, J. Dortmans, C. Weldon, R.D. Horansky, T.B.Meurs, C.-M. Wang, D.F. Williams, and C.L. Holloway, "Configuring and verifying reverberation chambers for testing cellular wireless devices," *IEEE Trans. Electromagn. Compat.*, vol. 58, no. 3, pp. 661–671, June, 2016.

[14] D. Fedeli, G. Gradoni, V.M. Primiani, & F. Moglie, "Accurate analysis of reverberation field penetration into an equipment-level enclosure" *IEEE Trans. Electromagn. Compat.*, vol. 51, pp. 170-180, May, 2009.

[15] K.A. Remley, R.J. Pirkl, H.A. Shah, & C.M. Wang, "Uncertainty from choice of mode-stirring technique in reverberation-chamber measurements," *IEEE Trans. on Electrom. Comp.*, vol. *55*, pp. 1022-1030, Dec., 2013.

[16] A. Gifuni, H. Khenouchi, and G. Schirinzi, "Performance of the reflectivity measurement in a reverberation chamber," *Prog. In Electromagn. Research PIER*, vol. 154, pp. 87–100, 2015.

[17] P. Corona, G. Latmiral, and E. Paolini, "Performance and analysis of a reverberating enclosure with variable geometry," *IEEE Trans. Electromagn. Compat.*, vol.22, pp. 2–5, Feb. 1980.

[18] D.A. Hill, "Electronic mode stirring for reverberation chambers," *IEEE Trans. on Electromagn. Compat.* vol. 36, pp. 294-299, Nov. 1994.

[19] T.A. Loughry, "Frequency stirring: an alternate approach to mechanical mode-stirring for the conduct of electromagnetic susceptibility testing," Phillips Lab., Rep. PL-TR-91-1036, 1991.

[20] A. Gifuni, "Probability density function of the quality factor for reverberation chambers operating with hybrid stirring including frequency stirring", *IEEE Trans. Electromagn. Compat.*, vol. 58, n. 3, pp. 919-922, June, 2016.

[21] A. Gifuni, "Effects of the correction for impedance mismatch on the measurement uncertainty in a reverberation chamber", *IEEE Trans. Electromagn. Compat.*, vol. 57, no. 6, pp. 1724-1727, Dec. 2015.

[22] J.G. Kostas, and B. Boverie, "Statistical model for a mode-stirred chamber," *IEEE Trans. Electromagn. Compat.*, vol.33, pp. 366-370, November 1991.

[23] A. Papoulis, "Probability, random variables and Stochastic Process," New York: McGraw-Hill, 1991.

[24] J.S. Bendant and A.G. Piersol, "Random data, analysis and measurement procedures," New York: John Wiley & Sons, 1986.

[25] C.F.M. Carobbi, "The statistical field uniformity criterion in transverse electromagnetic waveguides," *IEEE Trans. on Electromagn. Compat.*, vol. 59, pp. 2052-2053, Dec., 2017.

[26] P. Besnier, B. Demoulin, *Electromagnetic Reverberation Chambers*, Wiley-ISTE, August 2011.

[27] O.G. Richalot, S. Mengue, and O. Picon, "Statistical model of an undermoded reverberation chamber," *IEEE Trans. on Electromagn. Compat.*, vol. 48, pp. 248-251, Feb., 2006.

[28] L.R. Arnaut, "Limit distributions for imperfect electromagnetic reverberation," *IEEE Trans. on Electromagn. Compat.*, vol. 45, pp. 357-377, Aug., 2003.

[29] Primiani, V. M. and F. Moglie, "Numerical simulation of reverberation chamber parameters affecting the received power statistics," *IEEE Trans. on Electromagn. Compat.*, vol. 54, pp. 522-532, June, 2012.

[30] X. Chen, "Model selection for investigation of the field distribution in a reverberation chamber," *Prog. In Electromagn. Research M*, vol. 28, pp. 169–183, 2013.

[31] O.G. Richalot, S. Mengue, and O. Picon, "Statistical model of an undermoded reverberation chamber," *IEEE Trans. on Electromagn. Compat.*, vol. 48, pp. 248-251, Feb., 2006.

[32] P. Corona, G. Ferrara, and M. Migliaccio, "Reverberating chamber electromagnetic field in presence of an unstirred component," *IEEE Trans. on Electromagn. Compat.*, vol. 42, pp. 111-115, May 2000.

[33] C.L. Holloway, D.A. Hill, J.M. Ladbury, and G. Kapke, "Requirements for an effective reverberantion chamber:unloaded or loaded," *IEEE Trans. Electromagn. Compat.*, vol.48, pp.187-194, Feb. 2006.

[34] R. Serra, F. Leferink, and F. Canavero, "Good-but-imperfect electromagnetic reverberation in a VIRC," *in Proc. IEEE Int. Symp. Electromagn. Compat.*, Long Beach, CA, Aug. 2011, pp. 954–959.

[35] G. Gradoni, D. Micheli, F. Moglie, and V.M. Primiani, "Absorbing cross section in reverberation chamber: experimental and numerical results," *Prog. In Electromagn. Research B*, vol. 45, 187–202, 2012.

[36] K.A. Remley, R.J. Pirkl, C.M. Wang, D. Senic, A.C. Homer, M.V. North, M.G. Becker, R.D. Horansky, and C.L. Holloway, "Estimating and correcting the device-under-test transfer function in loaded reverberation chambers for over-the-air-tests," *IEEE Trans. Electromagn. Compat.*, DOI: 10.1109/TEMC.2017.27089852017.

[37] M. Barazzetta, D. Micheli, F. Moglie, and V.M. Primiani, "Over-the-air performance testing of a real 4G LTE base station in a reverberation chamber," *Electrom. Compat., IEEE Intern. Symp.* EMC, Raleigh, NC, USA, pp. 903-908 August 2014. DOI:10.1109/ISEMC.2014.6899096.

[38] V. Rajamani, C.F. Bunting, and J.C. West "Stirred-Mode operation of reverberation chambers for EMC testing," *IEEE Trans. Electromagn. Compat.*, vol.61, pp.2759-2764, Oct. 2012.

[39] X. Zhang, M. Robinson, I.D. Flintoft, and J.F. Dawson "Inverse Fourier transform technique of measuring averaged absorption cross section in the reverberation chamber and Monte Carlo study of its uncertainty," *Electrom. Compat., IEEE Intern. Symp.* EMC Europe, pp. 263-267, 2016, DOI:10.1109/EMCEurope.2016.7739161.

[40] L.R. Arnaut, "Effect of local stir and spatial averaging on measurement and testing in mode-tuned and mode-stirred reverberation chambers," *IEEE Trans. Electromagn. Compat.*, vol. 43, pp. 305-325, August 2001.